Expanding the pyridine-formic acid cocrystal landscape under extreme conditions

Rachael Lee,[a,b] Andrew J. Firbank, Michael R. Probert[b] and Jonathan W. Steed[a]*

a Department of Chemistry, Durham University, South Road, Durham, DH1 3LE, UK

b School of Chemistry, Newcastle University, Newcastle upon Tyne, NE1 7RU, UK

Pyridine and formic acid have been crystallized at differing ratios by both cryo-crystallization and compression in a diamond anvil cell. Mixtures of the liquids in 1:1, 1:2 and 1:4 ratios all crystallize at high pressure, while only the 1:1 and 1:4 compositions were crystallized by *in situ* low temperature capillary crystallization. The 1:2 structure crystallized by high pressure is a previously unknown cocrystal of pyridine - formic acid. For the 1:4 mixture, a new polymorph has been identified at a pressure of 14.2 kbar with a distinctly different structure and bonding pattern to that of the previously reported low temperature form.

Introduction

Polymorphism at high pressure (HP) is a concept which has been gaining interest, with drastic improvements in the equipment available over the past few decades. As a result, it is becoming a more common way to map a substance's structural and polymorphic behavior. While previously the realm of planetary scientists and geologists, high pressure crystallography is now more widespread as a technique.[1]

The crystallization of multiple polymorphs of a given substance depends on both kinetic and thermodynamic factors. Variation of temperature and pressure can significantly expand the solid form landscape; some polymorphs are stable only within a narrow range of temperatures and pressure, while others are only obtainable through the application of pressure to a liquid, solution, or existing single crystal which can undergo a phase transition.[2] Examples of compounds which exhibit polymorphism at high pressure or low temperature (LT) are the common simple molecules water,[3] acetone,[4] and benzene,[5] as well as more complex molecules such as 1-bromo-2,4,6-trifluorobenzene[6] and various amino acids.[7, 8]

Computational crystal structure prediction (CSP) has proven to be an effective tool at predicting crystal structure and polymorphism in some substances, and can give an indication of the existence of possible high-pressure polymorphs of a compound, which tend to fall in the higher density region of the energy-density landscape. Examples are 2-fluorophenylacetylene[9] and 2- and 4-chlorophenol,[10] all of which exhibit HP/LT polymorphism which is reflected in the CSP results. Additionally, the cholesterol drug Dalcetrapib is an excellent example of a high pressure polymorph that has been correctly predicted using CSP, despite the failure of initial crystallization attempts.[11] Knowing there is a high possibility of such a polymorph's existence, an experimenter is more likely to persist in screening, which is particularly relevant to the pharmaceutical industry where fast, high-throughput screening techniques are preferred. These may overlook, or fail to find, the precise crystallization conditions of a particular form. From CSP alone, without additional knowledge of the nature of HP/LT polymorphism, it is difficult to determine which structures can be accessed with high pressure. To address this shortcoming, it is useful to conduct further investigations into the subtle structural factors which contribute to polymorphism under different conditions.

We have recently shown that crystallization of 2- and 3-fluorotoluene under high pressure affords structures different from those obtained at low temperature (LT) as a result of the dominance of close packing effects at HP rather than the very weak H···F hydrogen bonding.[12] It is possible that the presence of a stronger, structure-defining hydrogen bond in such a system would reduce the likelihood of HP/LT polymorphism. However, even in the presence of dominant hydrogen bonding, polymorphism arising from varying arrangements of weaker interactions in the crystal remains a distinct possibility.[13]

Herein, we investigate a series of cocrystals composed of pyridine and formic acid. Of these, the structures of the 1:1 and 1:4 cocrystals have been previously reported at low temperature and ambient pressure.[14] Pyridine-formic acid is a system which displays a strong O-H···N hydrogen bond, however the degree of proton transfer can be manipulated by the addition of further equivalents of formic acid; as the relative concentration of polar components increases, the O-H···N bond gradually increases in strength until proton transfer occurs.[15] This results in a system with different bonding types and motifs to the original system, which may have a significant effect on HP/LT polymorphism of this series. The pyridine formic acid system was chosen for study due to its well-documented concentration dependent stoichiomorphism. Any deficiency in knowledge of the extent of their behavior and bonding capabilities can be seen as an oversight. Small molecule weak acid-base interactions are a classic example of a hydrogen bonding motif seen in supramolecular chemistry, and the pyridine-formic acid mixture presented a simple, and logical route to investigating such high pressure crystal structure landscapes.

Cocrystals have long been of significant interest to the scientific community, with numerous potential applications ranging from gas storage and separation,[16] non-linear optical materials[17] and the fine tuning and control of the properties of active pharmaceutical

ingredients.[18] The definition of what constitutes a cocrystal is under frequent scrutiny.[18-20] Generally, a cocrystal is a crystal containing two or more components. This definition breaks down when looking more closely at what those components are. It has been argued that any crystal containing a solvent molecule should not warrant the name cocrystal. This definition would exclude all solvates and hydrates from the class despite their being no conceptual difference between a solvate and a cocrystal containing components that have not been used as solvents.[21] Additionally, a salt containing an anion-cation pair does not qualify as a cocrystal because the components cannot be separated, however the position of a proton can be dependent on conditions and hence even this boundary is sometimes difficult to accurately define for a given system.[22] The scope of cocrystals is also sometimes restricted to crystals formed from reactants which are solid and neutral under ambient conditions.[23] However, application of high pressure to a liquid mixture frequently results in a liquid-solid phase transition to give a crystalline multi-component solid and in the present work we use the term to include all multi-component molecular crystals.

Experimental

New low temperature structures were obtained from *in situ* cryo-crystallization. Pyridine-formic acid mixtures were loaded into a 0.3 mm borosilicate glass capillary, which was sealed at both ends, attached to a pin and then mounted on the diffractometer. Both Bruker CCD SMART 6K and Agilent Xcalibur Gemini diffractometers were used each equipped with Oxford Cryosystems open flow nitrogen cryostats. A combination of cooling and flash freezing with liquid nitrogen was used to obtain a polycrystalline material, and crystals suitable for diffraction were obtained by temperature cycling just below the melting point of the crystals. Above the melting point, all the crystals returned to the liquid phase.

High pressure structures were obtained by *in situ* compression in a diamond anvil cell (DAC). A 0.25 mm thickness steel gasket, pre-indented to 0.15 mm, with a precision drilled 300 μm hole created the sample chamber between the two diamond anvils, of culet size 0.8 mm. A ruby chip was included in the sample chamber for pressure determination. Pressure was applied until the sample gave a polycrystalline material, at which point the pressure was cycled around the melting transition at ambient temperature to give a single crystal. Given that no solvent was used, the crystal could be grown to fill the entire sample chamber. The diamond anvil cell was directly attached to a goniometer head and mounted on the diffractometer. Data were collected using the XIPHOS II[24, 25] diffractometer at Newcastle University, a four-circle Bruker diffractometer with Ag-Kα *IμS* generator.[26] The pressure inside the cell was measured after equilibration by the R_1 ruby fluorescence method.[27] Data collection conditions are detailed in Table 1. HP data were collected beyond the phase boundary by over-pressurizing the cell to ensure the crystal remained stable during the experiment. On reduction of pressure, all crystals melted back to the liquid phase.

Data were handled in the Bruker APEX2[28] software suite with SAINT[29] and SADABS[30] used for integration, cell refinement and scaling. Dynamic masks were generated using the program ECLIPSE[31]. The Olex2[32] interface for the SHELX[33] program suite was used for structure solution and refinement. All hydrogen atoms on heteroatoms were located in Fourier difference maps.

Table 1. Conditions of pyridine (PY) – formic acid (FA) crystallization and data collection.

Ratio PY:FA	LT data set temperature (K)	HP measurement pressure (kbar)	HP crystal growth pressure (kbar)	HP initial occurrence of polycrystalline phase (kbar)

1:1	200	9.7 (2)	9.2 (2)	21.2 (2)
1:2	-	10.9 (2)	8.7 (2)	14.7 (2)
1:4	183	14.2 (2)	11.8 (2)	14.9 (2)

Results and Discussion

Pyridine and formic acid cocrystallize at HP in the ratios 1:1, 1:2 and 1:4. LT structures are already known for the 1:1 and 1:4 mixtures.[14] The 1:1 cocrystal adopts the same form at both LT and at HP (9.2 GPa); however different polymorphs were obtained for the 1:4 mixture at LT (200 K) and HP (14.2 kbar). No LT form could be isolated for the 1:2 mixture.

Pyridine Formic acid 1:1

A 1:1 mixture of pyridine and formic acid crystallizes in space group $P2_1/n$. The crystals obtained from pressurization and cryo-crystallization adopt the same crystal packing arrangement, the principal structural difference being the packing density which was markedly higher for the HP phase (Table 4). The primary intermolecular interaction is an O-H···N hydrogen bond with a donor-acceptor distance of 2.663(3) Å in the LT structure. The structure exhibits π-π stacking between equivalent pyridine molecules along the *b* axis. Defining a plane across individual molecules shows a centroid-centroid distance of 3.817(3) Å. These centroids are offset from each other by 1.32(2) Å relative to the plane of the ring. Adjacent stacks are offset from each other and form a layered motif in the *c* axis, with alternating layers of formic acid and pyridine molecules (Fig. 1).

HP data for the 1:1 cocrystal were collected at 9.71 kbar. This was an over-pressurization to prevent the crystal melting during data collection. Despite being the same polymorph, the structure at HP exhibits some changes in packing as a result of the applied pressure. The O-

H···N hydrogen bond is compressed to a donor-acceptor distance of 2.63(1) Å. Similarly, the pyridine rings are forced closer together with the ring planes having a centroid-centroid distance of 3.647(1) Å with an offset of 1.240(4) Å. A summary of the hydrogen bonding is given in Table 2.

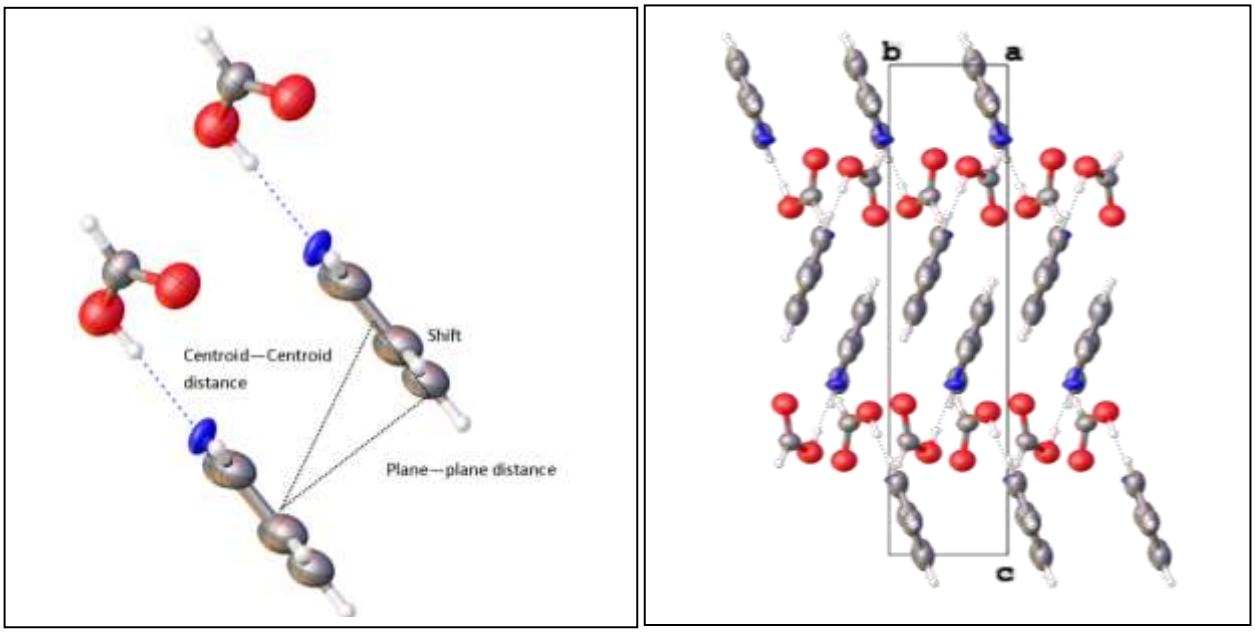

Figure 1. (Left) Stacking between pyridine rings showing how key parameters are defined. (Right) View down the *a* axis of pyridine formic acid 1:1, showing layers extending in the *c* axis direction.

Table 2. Hydrogen bond details for the unique hydrogen bond in a 1:1 cocrystal of pyridine formic acid.

Contact	Low temperature	High pressure
H-A (Å)	1.69(4)	1.81(1)
D-A (Å)	2.663(3)	2.63(1)
D-H (Å)	0.98(4)	0.82(1)
D-H-A (°)	172(4)	176.9(7)

Pyridine-Formic acid 1:2

The pyridine - formic acid 1:2 cocrystal was found to crystallize only by pressurization of the liquid mixture; capillary crystallization at LT afforded only a glass. The asymmetric unit contains one pyridinium ion, a formate ion and a formic acid molecule. Hence the structure is strictly a salt cocrystal of formic acid and pyridinium formate. The shortest intermolecular

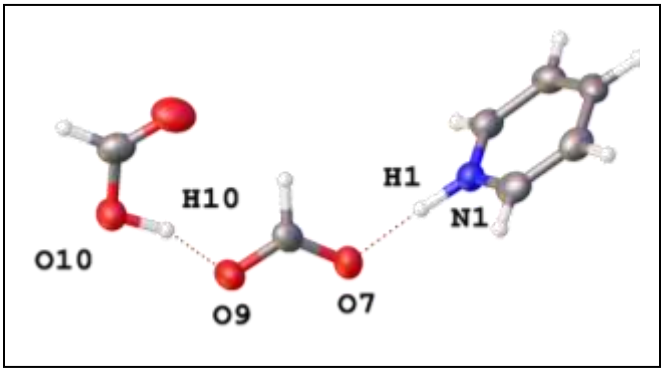

contacts comprise both N-H···O and O-H···O hydrogen bonds in a short chain of hydrogen interactions, shown in Figure 2.

Figure 2. Asymmetric unit of pyridine-formic acid 1:2 (HP) showing the primary hydrogen bonding motif.

The pyridinium-formate interaction has a donor-acceptor distance of 2.647(3) Å (see

Table 3), compared to 2.634(12) for the HP 1:1 cocrystal. There is little difference in the N···O distances between the two structures, despite a significant change in the nature of the hydrogen bond between the molecules. The N-H···O and C-H···O interactions form a cyclic bonding motif confined to a single plane, as shown in Figure 3. The angle between the plane of

the pyridinium ion, and the formate/formic acid pair is such that the hydrogen bonding network is propagated in three dimensions. Further interactions occur between the formate ion and the

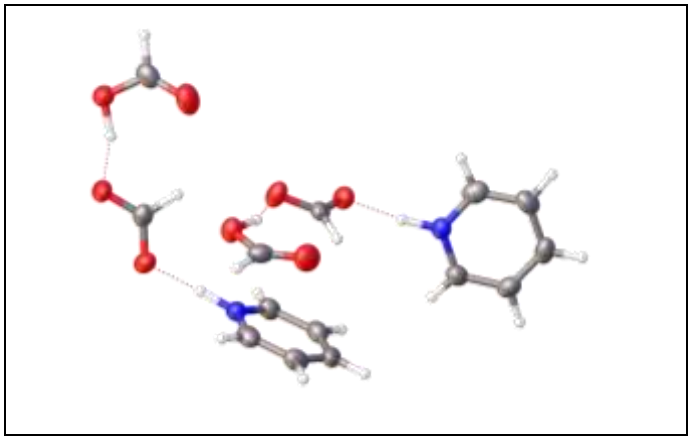

edge of the pyridinium ion, with each of the oxygen atoms exhibiting two C-H···O interactions. The formic acid – formate charge-assisted hydrogen bond has D-A O···O distance of 2.458(4) Å. The O-H bond of the formic acid is 1.05(6) Å, slightly longer than a conventional OH bond, indicating that the proton is partially shared between the two molecules, without any apparent disorder between two distinct positions.

Figure 3. Hydrogen bonding interactions between pyridinium and formate ions in the HP 1:2 structure.

An analogous structure of a pyridine - oxalic acid cocrystal has been reported which crystallizes as dipyridinium bis(hydrogen-oxalate) oxalic acid, in which the pyridinium ion is hydrogen bonded to the hydrogen oxalate ion.[34] The primary hydrogen bond has a D-H distance of 1.00(3) Å, HA distance 1.97(3) Å and DA distance 2.792(3) Å. The longer bond distance indicates a slightly weaker interaction, which is consistent with the larger size and hence greater delocalization of the negative charge on the hydrogen oxalate anion compared with the formate ion in the pyridine-formic acid structure.

Table 3. Details of N1-H1···O7 hydrogen bond contact in the high pressure structure of 1:2 pyridine-formic acid.

Contact	High Pressure
H-A (Å)	1.62(4)
D-A (Å)	2.647(3)
D-H (Å)	1.04(3)
Angle (°)	171(4)

Pyridine formic acid 1:4

As in the case of the 1:1 cocrystal, a 1:4 mixture of pyridine and formic acid crystallizes under both HP and LT conditions. In this case, however, different polymorphs are obtained via the two methods. The LT form crystallizes in orthorhombic space group $Pca2_1$, while in the HP form, the symmetry is reduced, giving space group $P2_1$. Figure 4 shows the view down the *a* axes for both the HP and LT polymorphs.

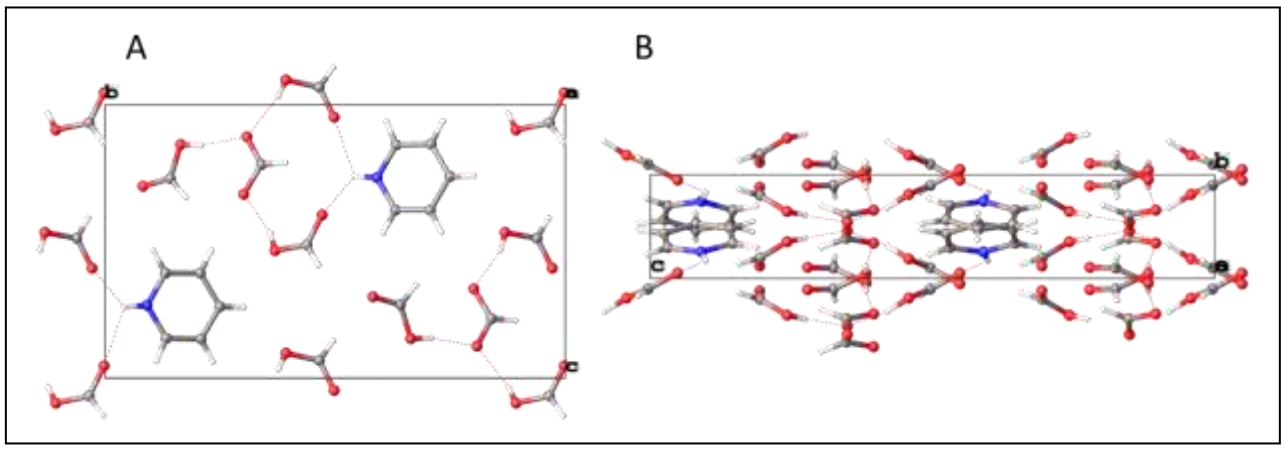

Figure 4. View down the *a* axis of the 1:4 adduct. a) High pressure and b) low temperature.

Both forms contain a pyridinium ion, with one formate ion and three formic acid molecules (Figure 5). In the LT form, there are two novel hydrogen bonds between the pyridinium hydrogen atom and two neighboring carbonyl oxygen atoms of formic acid molecules with D-A distances 2.870(3) and 3.019(4) Å. One of these formic acid molecules is 'bridging' a C-N bond in the pyridinium ring, with an O-H···H-C hydrogen bond adjacent to the C=O···H-N primary interaction. In the HP polymorph, this interaction is altered; there are still two hydrogen bonds involving the pyridinium N-H, but no seven-membered-ring style bonding pattern which is present in the LT form. These two interactions are with two carbonyl oxygen atoms from formic acid with D-A distances 2.853(10) and 3.105(9) Å.

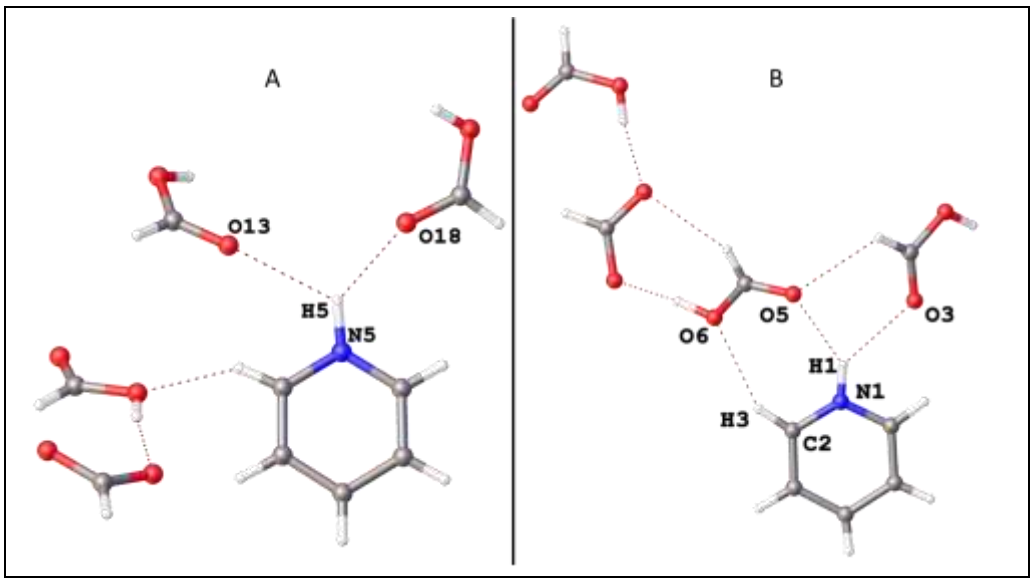

Figure 5. Asymmetric units of a) high pressure and b) low temperature polymorphs of pyridinium formate tris(formic acid).

The strong directional hydrogen bond which dominates the packing of the 1:1 structure is lengthened at the higher ratio of formic acid and HP. As proton transfer has occurred, the ion-ion interaction between pyridinium and formate ions becomes more dominant. Charge assisted hydrogen bond interactions are still seen in both LT and HP 1:4 structures, but are weaker with longer bond distances, more oblique angles and bifurcated hydrogen bonding.

Ion-ion interactions are comparable in strength to covalent bonds with bond strengths 100-350 kJ mol^{-1}. Hydrogen bonds are weaker with strengths in the range 4-60 kJ mol^{-1} but are highly directional. The N···HO hydrogen bond in the 1:1 pyridine formic acid cocrystal qualifies as a moderate electrostatic hydrogen bond based on the D-A distances of 2.663(3) Å and 2.634(12) Å for the LT and HP versions, respectively.[35, 36] The distance of the charge assisted hydrogen bond in the 1:2 salt cocrystal is comparable at 2.647(3) Å. In the 1:4 case, for the LT polymorph, the $NH^{+}\cdots O^{-}$ bond has a D-A distance 2.870(3) Å. For the HP polymorph, the closest hydrogen contact is 2.853(10) Å. Close packing effects have greater dominance over the structure, and the components adopt a conformation which gives the structure a higher packing efficiency than the LT polymorph. A comparison of the occupied space calculated using the OLEX2 package for all structures is given in Table 4. In all cases, the higher pressure structure has the higher density packing.

There are π-π stacking interactions present in both polymorphs of the 1:4 mixture and as expected, the minimum distance between pyridine rings in the HP structure, 3.560(1) Å, is shorter than the distance of 3.702(3) Å observed in the LT polymorph. The offset between the rings is also slightly smaller in the HP phase.

Table 4. Percentage of unit cell occupied by Py-FA structures.

Table 5. Summary of Crystallographic data.

Ratio	Low temperature	High pressure
1:1	67.51	72.13
1:2	-	76.36
1:4	69.36	73.66

	1:1 LT[14]	1:1 HP	1:2 HP	1:4 LT[14]	1:4 HP
Empirical formula	$C_6H_7NO_2$	$C_6H_7NO_2$	$C_7H_9NO_4$	$C_9H_{18}NO_8$	$C_9H_{13}NO_8$
T / K	173	295	295	183	295
P / kbar	ambient	9.2(2)	10.9(2)	ambient	14.2(2)
Crystal system	Monoclinic	Monoclinic	Monoclinic	Orthorhombic	Monoclinic
Space group	$P2_1/n$	$P2_1/n$	$P2_1/n$	$Pca2_1$	$P2_1$
a / Å	10.954(6)	10.760(2)	7.4036(4)	16.35(1)	3.560(1)
b / Å	3.817(3)	3.647(1)	13.380(2)	3.702(3)	16.533(5)
c / Å	15.842(7)	15.549(5)	8.2074(6)	20.23(1)	9.798(2)
β / °	104.96(5)	104.15(2)	114.05(1)	90	93.78(1)
Z	4	4	4	4	2
V / Å^3	639.9(7)	591.6(2)	742.5(1)	1224.5	575.4(2)
D_c / gcm^{-3}	1.30	1.41	1.53	1.43	1.52
Unique reflns.	1120	5497	6501	1835	2638
Completeness %	-	42	66	-	50
$R1$	0.047	0.071	0.050	0.041	0.041
$wR2$	0.167	0.209	0.134	0.114	0.093
GooF	-	1.17	1.05	-	1.08

Proton transfer

As the proportion of formic acid present in the mixture reaches two equivalents, proton transfer occurs in the crystal structure, and persists as the ratio increases further. It has been previously reported that for such a hydrogen bonded system, increasing the acid:base ratio strengthens the AH···B bond to the point of proton transfer.[37] There is evidence for this process also occurring in solution. In a low temperature NMR study of a pyridine-acetic acid mixture, increasing the relative concentration of acetic acid was found by Smirnov *et al.* to favor protonation of pyridine, although this could only be seen at temperatures below 120 K due to the high rate of proton exchange at ambient temperature.[38] This effect can be seen in the solid state also, in the pyridine-formic acid series; proton transfer occurs in the 1:2 adduct, with a N^+-H bond distance of 1.04(3)Å. In the 1:4 LT adduct, this bond has decreased in length to 0.87(5) Å, implying that the presence of an additional two formic acid molecules in the immediate environment further promotes the O-H-N proton transfer further localizing the proton on the nitrogen atom. This effect warrants further investigation by single crystal neutron diffraction in order to fully resolve the hydrogen atom positions. Table 6 shows the bond distances for the primary pyridine-formic acid or pyridinium-formate hydrogen bond for each structure. It is notable that the donor and acceptor atoms change as proton transfer takes place.

Table 6. Hydrogen bond parameters for pyridine-formic acid series.

Ratio	D	H	A	DH/Å	HA/Å	DA/Å	DHA/°
1:1 HP	O7	H7	N1	0.821(8)	1.814(9)	2.634(12)	176.9(7)
1:2 HP	N1	H1	O7	1.04(4)	1.62(4)	2.647(3)	171(4)
1:4 LT	N1	H1	O7	0.87(5)	2.14(5)	2.870(3)	141(4)
1:4 HP	N5	H5	O18	0.99(8)	2.08(6)	2.853(10)	134(4)

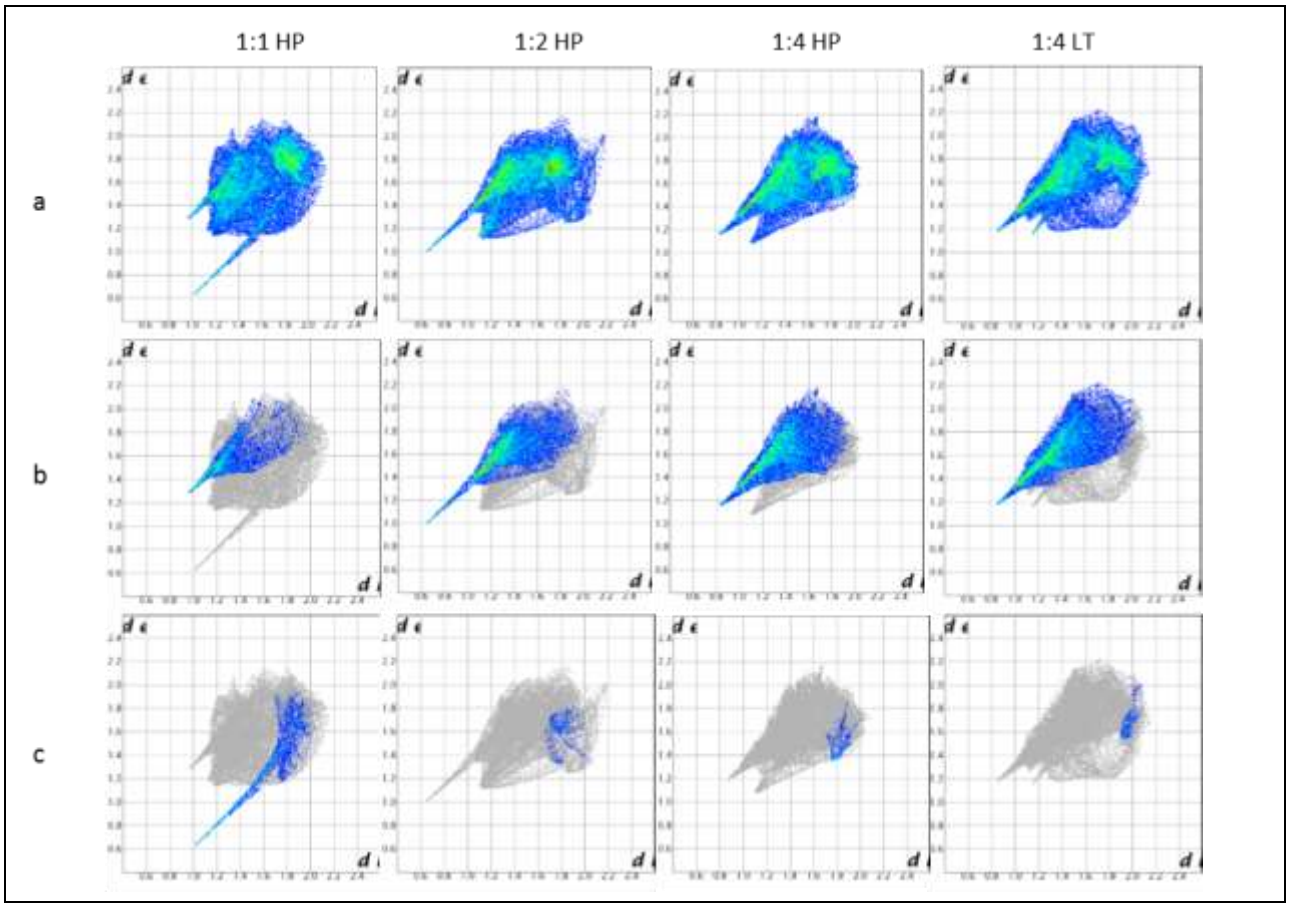

Figure 6. Hirshfeld 2D fingerprint plots of 1:1, 1:2, 1:4 HP and 1:4 LT crystal structures of pyridine-formic acid. a) Whole surface, b) OH interactions, c) NH interactions.

A useful tool for the analysis of the intermolecular contacts in a crystal structure is offered by the program Crystal Explorer, which can be used to generate Hirshfeld surfaces for molecules and also provides a 2D representation of these contacts called 'fingerprint plots'.[39, 40] The compression of crystal structures at high pressure has been analyzed in this way and shows the typical differences between LT and HP structures. HP fingerprint plots tend to be more compressed, as contacts within the structures are also compressed, as well as tending towards

higher symmetry about the $d_i = d_e$ diagonal.[41] Surfaces and fingerprint plots were generated for the pyridine/pyridinium in each of the structures 1:1, 1:2, 1:4 HP and 1:4 LT where d_e is the distance between the Hirshfeld surface and nearest contact external to the surface, and d_i is the same but internal to the surface, shown in Figure 6.

For the 1:1 structure, the large peak on the lower part of the fingerprint plot is the result of the prominent O-H···N hydrogen bond. There is also a weaker interaction between C-H groups of the ring and an oxygen atom of formic acid which creates the smaller peak on the left of the fingerprint plot. This interaction accounts for 14% of the generated surface, and includes contributions from more than one C-H···O contact. The bulk of the points in the plot are from H···H interactions.

The H···O plots in Figure 5 shows clearly how different the interactions are in the 1:2 structure compared to the 1:1. The extended region on the left of the fingerprint plot represents all H···O interactions, accounting for 37% of the total surface interaction. This includes both the charge assisted hydrogen bond and all C-H···O contacts, which cannot be separated in this type of analysis.

For the 1:4 HP structure, the main peak in the fingerprint plot arises from O···H interactions. However, compared to the 1:2 fingerprint plot, this peak occurs at greater *de*, showing that the nearest contacts to the pyridinium proton are further away than for the 1:2 structure. This type of interaction accounts for 44% of the pyridinium surface interactions; a higher contribution than for the other two structures but also at greater distance from the pyridinium ion.

The LT polymorph of the 1:4 mixture has a different bonding pattern to that of the HP polymorph. In the fingerprint plot, the main peak on the left represents the H···O contacts,

accounting for 46% of the surface. The large diffuse region at d_e ~1.2 is largely from H···H contacts. This region is compressed in the HP structure fingerprint plot, as the molecules are more closely packed and therefore have shorter atom to atom contacts.

Conclusions

We have shown that similar systems, comprised of the same components can have very different responses to high pressure and low temperature crystallization.

The 1:2 mixture of pyridine and formic acid gives a glass on flash freezing and temperature cycling in a capillary, while application of HP affords a previously unreported salt cocrystal containing a charge-assisted hydrogen bond.

The 1:4 mixture of the same components exhibits LT/HP polymorphism, and adopts distinctly different structures under the two sets of conditions. It is clear that one contribution to this difference is the less directional hydrogen bonding in the 1:4 mixture, which allows close packing of molecules to have a greater effect, and a new polymorph to form when the components are compressed to high pressure, resulting in shorter atom-to-atom contacts and higher crystal density. The presence of such an interaction in the 1:1 mixture contributes to the structure's stability with regards to extreme conditions, enabling this system to maintain the same phase across the explored conditions.

We have also shown that where cryo-crystallization is ineffective, a crystal structure may still be obtained by application of high pressure, and that the fingerprint plots of Hirshfeld surface interactions can easily highlight the prominence of particular interactions across different phases. This is evidence that a polymorph of a compound may exist only at pressures beyond ambient conditions, which may be predicted by CSP methods where time- consuming practical methods are unsuitable, such as screening for polymorphs of an active pharmaceutical ingredient.

Additionally, where CSP results identify a possible a low energy polymorph that cannot be isolated by traditional crystallization methods, HP crystallization may represent an alternative route to isolation of novel solid forms.[11]

Acknowledgements

We thank Bruker UK Limited for funding.

Notes and references

(1) Lee, R.; Howard, J. A. K.; Probert, M. R.; Steed, J. W., Structure of organic solids at low temperature and high pressure. *Chem. Soc. Rev.* **2014,** 43, (13), 4300-4311.
(2) Boldyreva, E., High-pressure diffraction studies of molecular organic solids. A personal view. *Acta Crystallogr. Sect. A* **2008,** 64, (1), 218-231.
(3) Petrenko, V. F.; Whitworth, R. W., *Physics of Ice*. ed.; Clarendon Press: 1999.
(4) R. Allan, D.; J. Clark, S.; M. Ibberson, R.; Parsons, S.; R. Pulham, C.; Sawyer, L., The influence of pressure and temperature on the crystal structure of acetone. *Chem. Commun.* **1999**, (8), 751-752.
(5) Fourme, R.; Andre, D.; Renaud, M., A redetermination and group-refinement of the molecular packing of benzene II at 25 kilobars. *Acta Crystallogr. Sect. B* **1971,** 27, (6), 1275-1276.
(6) Probert, M. R.; Chung, Y. H. P.; Howard, J. A. K., Two solid state phases of 1-bromo-2,4,6-trifluorobenzene, crystallised under non-ambient conditions. *CrystEngComm* **2010,** 12, (9), 2584-2586.
(7) Minkov, V. S.; Tumanov, N. A.; Cabrera, R. Q.; Boldyreva, E. V., Low temperature/high pressure polymorphism in dl-cysteine. *CrystEngComm* **2010,** 12, (9), 2551-2560.
(8) Moggach, S. A.; Parsons, S.; Wood, P. A., High-pressure polymorphism in amino acids. *Crystallogr. Rev.* **2008,** 14, (2), 143-184.
(9) Ridout, J.; Price, L. S.; Howard, J. A. K.; Probert, M. R., Polymorphism Arising from Differing Rates of Compression of Liquids. *Cryst. Growth Des.* **2014,** 14, (7), 3384-3391.
(10) Oswald, I. D. H.; Allan, D. R.; Day, G. M.; Motherwell, W. D. S.; Parsons, S., Realizing Predicted Crystal Structures at Extreme Conditions: The Low-Temperature and High-Pressure Crystal Structures of 2-Chlorophenol and 4-Fluorophenol. *Cryst. Growth Des.* **2005,** 5, (3), 1055-1071.
(11) Neumann, M. A.; van de Streek, J.; Fabbiani, F. P. A.; Hidber, P.; Grassmann, O., Combined crystal structure prediction and high-pressure crystallization in rational pharmaceutical polymorph screening. *Nat Commun* **2015,** 6.
(12) Ridout, J.; Probert, M. R., High-Pressure and Low-Temperature Polymorphism in C–H···F–C Hydrogen Bonded Monofluorotoluenes. *Cryst. Growth Des.* **2013,** 13, (5), 1943-1948.
(13) Fucke, K.; Qureshi, N.; Yufit, D. S.; Howard, J. A. K.; Steed, J. W., Hydrogen Bonding Is Not Everything: Extensive Polymorphism in a System with Conserved Hydrogen Bonded Synthons. *Cryst. Growth Des.* **2010,** 10, (2), 880-886.

(14) Wiechert, D.; Mootz, D., Molecular Beside Ionic: Crystal Structures of a 1/1 and a 1/4 Adduct of Pyridine and Formic Acid. *Angew. Chem.-Int. Edit.* **1999,** 38, (13-14), 1974-1976.
(15) Drichko, N. V.; Kerenskaia, G. Y.; Schreiber, V. M., Medium and temperature effects on the infrared spectra and structure of carboxylic acid–pyridine complexes: acetic acid. *J. Mol. Struct.* **1999,** 477, (1–3), 127-141.
(16) Jones, J. T. A.; Hasell, T.; Wu, X.; Bacsa, J.; Jelfs, K. E.; Schmidtmann, M.; Chong, S. Y.; Adams, D. J.; Trewin, A.; Schiffman, F.; Cora, F.; Slater, B.; Steiner, A.; Day, G. M.; Cooper, A. I., Modular and predictable assembly of porous organic molecular crystals. *Nature* **2011,** 474, (7351), 367-371.
(17) Huang, K.-S.; Britton, D.; late Margaret C. Etter, t.; Byrn, S. R., A novel class of phenol-pyridine co-crystals for second harmonic generation. *J. Mater. Chem.* **1997,** 7, (5), 713-720.
(18) Steed, J. W., The role of co-crystals in pharmaceutical design. *Trends Pharmacol Sci* **2013,** 34, (3), 185-193.
(19) Desiraju, G. R., Crystal and co-crystal. *CrystEngComm* **2003,** 5, (82), 466-467.
(20) Dunitz, J. D., Crystal and co-crystal: a second opinion. *CrystEngComm* **2003,** 5, (91), 506-506.
(21) Barbour, L. J.; Das, D.; Jacobs, T.; Lloyd, G. O.; Smith, V. J., *Supramolecular Chemistry: From Molecules to Nanomaterials*. ed.; John Wiley & Sons, Ltd: 2012.
(22) Aakeröy, C. B.; Fasulo, M. E.; Desper, J., Cocrystal or Salt: Does It Really Matter? *Mol. Pharm.* **2007,** 4, (3), 317-322.
(23) Aakeroy, C. B.; Salmon, D. J., Building co-crystals with molecular sense and supramolecular sensibility. *CrystEngComm* **2005,** 7, (72), 439-448.
(24) Probert, M. R.; Robertson, C. M.; Coome, J. A.; Howard, J. A. K.; Michell, B. C.; Goeta, A. E., The XIPHOS diffraction facility for extreme sample conditions. *J. Appl. Crystallogr.* **2010,** 43, (6), 1415-1418.
(25) Probert, M. R.; Coome, J. A.; Goeta, A. E.; Howard, J. A. K., Silver the new gold standard for high-pressure single crystal X-ray diffraction. *Acta Crystallogr. Sect. A* **2011,** 67, (a1), C528.
(26) Schulz, T.; Meindl, K.; Leusser, D.; Stern, D.; Graf, J.; Michaelsen, C.; Ruf, M.; Sheldrick, G. M.; Stalke, D., A comparison of a microfocus X-ray source and a conventional sealed tube for crystal structure determination. *J. Appl. Crystallogr.* **2009,** 42, (5), 885-891.
(27) Piermarini, G. J.; Block, S.; Barnett, J. D.; Forman, R. A., Calibration of the pressure dependence of the R[sub 1] ruby fluorescence line to 195 kbar. *J. Appl. Phys.* **1975,** 46, (6), 2774-2780.
(28) *APEX2*, 1.08; Bruker AXS Inc.: Madison, WI, 2004.
(29) *SAINT*, Bruker AXS Inc.: Madison, WI, 2007.
(30) *SADABS*, Bruker AXS Inc.: Madison, WI, 2001.
(31) Parsons, S., ECLIPSE In ed.; Edinburgh, UK, 2010.
(32) Dolomanov, O. V.; Bourhis, L. J.; Gildea, R. J.; Howard, J. A. K.; Puschmann, H., OLEX2: a complete structure solution, refinement and analysis program. *J. Appl. Crystallogr.* **2009,** 42, (2), 339-341.
(33) Sheldrick, G. M., SHELXL. *Acta Crystallogr., Sect. A: Found. Crystallogr.* **2008**, (A64).
(34) Newkome, G. R.; Theriot, K. J.; Fronczek, F. R., Dipyridinium bis(hydrogen oxalate)-oxalic acid. *Acta Crystallogr. Sect. C-Cryst. Struct. Commun.* **1986,** 42, (11), 1539-1541.
(35) Steed, J. W.; Atwood, J. L., *Supramolecular Chemistry*. 2nd ed.; John Wiley & Sons: Chichester, 2009.

(36) Jeffrey, G. A., *An Introduction to Hydrogen Bonding*. ed.; Oxford University Press: 1997.
(37) Balevicius, V.; Bariseviciute, R.; Aidas, K.; Svoboda, I.; Ehrenberg, H.; Fuess, H., Proton transfer in hydrogen-bonded pyridine/acid systems: the role of higher aggregation. *PCCP Phys. Chem. Chem. Phys.* **2007,** 9, (24), 3181-3189.
(38) Smirnov, S. N.; Golubev, N. S.; Denisov, G. S.; Benedict, H.; Schah-Mohammedi, P.; Limbach, H.-H., Hydrogen/Deuterium Isotope Effects on the NMR Chemical Shifts and Geometries of Intermolecular Low-Barrier Hydrogen-Bonded Complexes. *J. Am. Chem. Soc.* **1996,** 118, (17), 4094-4101.
(39) Spackman, M. A.; Jayatilaka, D., Hirshfeld surface analysis. *CrystEngComm* **2009,** 11, (1), 19-32.
(40) Spackman, M. A.; McKinnon, J. J., Fingerprinting intermolecular interactions in molecular crystals. *CrystEngComm* **2002,** 4, (66), 378-392.
(41) Wood, P. A.; McKinnon, J. J.; Parsons, S.; Pidcock, E.; Spackman, M. A., Analysis of the compression of molecular crystal structures using Hirshfeld surfaces. *CrystEngComm* **2008,** 10, (4), 368-376.

For Table of Contents use only

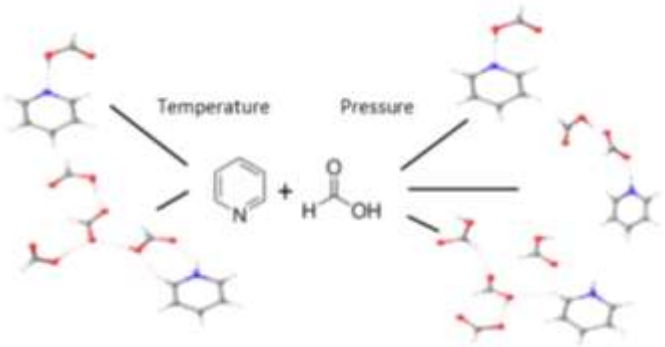

Synopsis

Concentration dependent high pressure – low temperature polymorphism is revealed in a pyridine – formic acid system by *in situ* cryo-crystallisation and compression by diamond anvil cell.